
Computer simulations and experimental studies of gel mobility patterns for weak and strong non-cooperative protein binding to two targets on the same DNA: application to binding of Tet repressor variants to multiple and single *tet* operator sites

Christoph Kleinschmidt¹, Karlheinz Tovar and Wolfgang Hillen*

Lehrstuhl für Mikrobiologie, Friedrich-Alexander Universität Erlangen-Nürnberg, Staudtstrasse 5, D-8520 Erlangen and ¹Max-Planck-Institut für Ernährungsphysiologie, 4600 Dortmund, FRG

Received December 21, 1990; Revised and Accepted February 6, 1991

ABSTRACT

A series of computer simulations of gel patterns assuming non-cooperative binding of a protein to two targets on the same DNA fragment was performed and applied to interpret gel mobility shift experiments of Tet repressor-*tet* operator binding. While a high binding affinity leads to the expected distribution of free DNA, DNA bound by one repressor dimer and DNA bound by two repressor dimers, a lower affinity or an increased electrophoresis time results in the loss of the band corresponding to the singly occupied complex. The doubly occupied complex remains stable under these conditions. This phenomenon is typical for protein binding to DNA fragments with two identical sites. It results from statistical disproportionation of the singly occupied complex in the gel. The lack of the singly occupied complex is commonly taken to indicate cooperative binding, however, our analysis shows clearly, that cooperativity is not needed to interpret these results. Tet repressor proteins and small DNA fragments with two *tet* operator sites have been prepared from four classes of tetracycline resistance determinants. The results of gel mobility shift analyses of various complexes of these compounds confirm the predictions. Furthermore, calculated gel patterns assuming different gel mobilities of the two singly occupied complexes show discrete bands only if the electrophoresis time is shorter than the inverse of the microscopic dissociation rate constant. Simulations assuming increasing dissociation rates predict that the two bands first merge into one, which then disappears. This behavior was verified by gel mobility analyses of Tet repressor-*tet* operator titrations at increased salt concentrations as well as by direct footprinting of the complexes in the gel. It is concluded that comparison

of the intensities of the single and the double occupation bands allow a rough estimation of the dissociation rate constant. On this basis the sixteen possible Tet repressor-*tet* operator combinations can be ordered with decreasing binding affinities by a simple gel shift experiment. The implications of these results for gel mobility analyses of other protein-DNA complexes are discussed.

INTRODUCTION

Native polyacrylamide gel electrophoresis has become a widely used method to detect and analyze protein-DNA complexes. It was introduced by Garner and Revzin (1) and Fried and Crothers (2) and was subsequently used to study many different interactions. A phenomenological theory of this method aiding in the interpretation of many of the experimental data published so far has been described recently (3). In particular, strong and weak binding to single operator sites and cooperative binding to multiple operator sites have been analyzed in detail. We are studying Tet repressor binding to two *tet* operators on the same DNA fragment by gel mobility analysis and wish to explain the results by a binding scheme as simple as possible. Therefore, we simulated the electrophoretic band patterns for strong and weak non-cooperative binding of a protein to two sites on the same DNA fragment by a numerical procedure. All predictions were then tested by respective experiments using the tetracycline regulatory elements.

Tetracycline resistance determinants in gram negative bacteria often encode a membrane protein which actively exports the drug from the resistant cell (4). These determinants can be grouped in five different classes named A through E (5, 6), which

* To whom correspondence should be addressed

represent sequence variants of each other (7, 8, 9, 10, 11). The expression of all these determinants is strictly regulated via a tetracycline sensitive repressor protein and two consecutive operators on the level of transcription (12, 13). Owing to variations in their primary structures these regulatory elements constitute a set of protein-DNA recognition mutants. It has been shown *in vivo* and *in vitro* that the efficiency of heterologous and homologous repressor-operator recognition among classes A through D varies substantially (14, 15). In this article we describe the analysis of all sixteen possible combinations of protein-DNA binding from these four classes by gel electrophoresis.

MATERIALS AND METHODS

Tet repressor and *tet* operator DNA purification

Tet repressor proteins of the resistance classes A, B, and C were purified from overproducing *E. coli* strains according to published procedures (7, 17, 18). The class D Tet repressor was purified from an overproducing strain (to be described elsewhere) by a published protocol (11). A detailed description of the DNA fragments and their purification has been published recently (16).

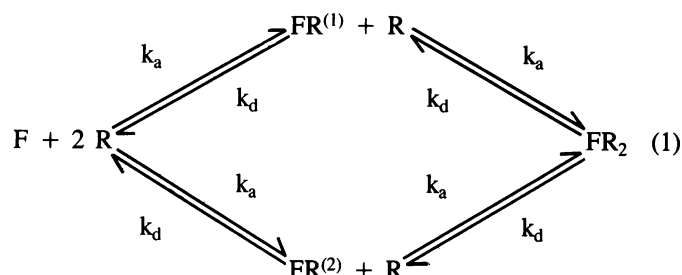
DNA binding and footprinting assay

The binding of Tet repressors to *tet* operator fragments were assayed by the gel mobility shift method as introduced by Garner and Revzin (1) and Fried and Crothers (2). Between 5 μ l and 20 μ l of binding reaction mixtures containing gel buffer (60 mM Tris base, 60 mM boric acid, 1 mM EDTA) and 6% to 12% glycerol were loaded onto preelectrophoresed 16 cm long, 1 mm thick, 5% or 10% polyacrylamide gels containing 60 mM Tris base, 60 mM boric acid, 1 mM EDTA, 10% glycerol. Electrophoresis was carried out in the same buffer at voltages between 2.5 V/cm and 10 V/cm at 20°C. In cases where sodium chloride was added to the gel and the electrophoresis buffers, the electrophoresis buffer was constantly exchanged between the chambers. The gels were either autoradiographed or stained with ethidium bromide to visualize DNA bands. For these experiments four restriction fragments, with sizes between 78 bp and 86 bp, containing the wildtype tandem *tet* operators O₁ and O₂ of tetracycline resistance classes A, B, C, and D (5), constructed and purified as described previously (16), were used. Another 124 bp long *EcoRI* fragment, containing two synthetic 19 bp long class B *tet* operators O₁ and O₂ with a distance of 42 bp between their palindromic centers was constructed by insertion of a 19 bp class B *tet* operator O₁ into the *Clal* site of pWH875 (19), after filling in the protruding ends of the *Clal* site. For large scale preparation the 124 bp *EcoRI* fragment was isolated and inserted into the unique *EcoRI* site of pWH802 to yield pWH934 and purified as described (16). This fragment was labelled at the 5' ends using T4 polynucleotide kinase, cut with *KpnI*, and the resulting 112 bp fragment was eluted from a polyacrylamide gel. After separating the repressor-operator complexes in native electrophoresis as described above, the DNA fragments were partially digested within the acrylamide matrix by the nuclease activity of 1,10-phenanthroline-copper as previously described (20), eluted from the gel and separated on sequencing gels.

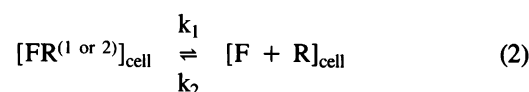
Theoretical model

The formulation of the model is based on the fundamental work of Cann (3,26,27). We assumed the non-cooperative binding of a repressor protein R to a DNA fragment F containing two

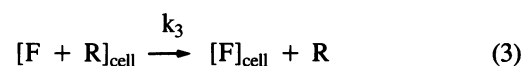
repressor binding sites (operators). In solution the following reactions are involved:



The microscopic rate constants k_a and k_d are considered to be equal for both binding sites and are not altered by the occupation of the respective other site. On polyacrylamide gels weak complexes show an unexpected stability (2). This is explained by the 'cage effect', namely the retarding influence of the gel matrix on the macroscopic, i.e. observable rate constants. According to the theoretical formulation given by Cann (3), the dissociation of an repressor-operator complex proceeds via an intermediate state in which the molecules are dissociated microscopically, but are still confined to the same 'cell' in the gel:



For a complete (macroscopic) dissociation the protein has to escape from this cell:

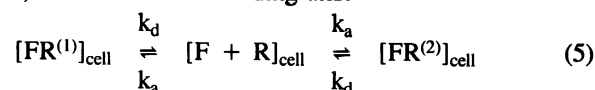


The diffusion of the DNA fragment is neglected because of its small diffusion coefficient. k_1 is identical to the microscopic dissociation constant k_d and k_2 has the same numerical value as k_a but is a first-order rate constant. k_3 is the rate constant for the escape from a cell in the gel, which is determined by the cell shape and the diffusion coefficient of the protein.

Under the condition $k_2 \gg k_3$, which is fulfilled throughout this work (see below), the macroscopic dissociation of a repressor-operator complex in the gel proceeds with the first-order rate constant

$$k_d \times (k_3/k_2) \quad (4)$$

(3). Since the gel matrix does not affect the free energy assigned to the binding reaction and, thus, does not change the equilibrium conditions, the macroscopic association rate is obtained by multiplication of k_a by the same factor (k_3/k_2). Since k_2 has the same numerical value as k_a , the macroscopic association rate has always the value of k_3 , but is second-order. We introduced the cage effect in our model calculations by slowing down all reactions in scheme (1) by the factor (k_3/k_2). However, due to the special situation of two binding sites on one DNA fragment, there is one reaction path which is not inhibited by the gel cage: the release of the repressor from a single occupied fragment ($FR^{(1)}$ or $FR^{(2)}$) and the subsequent reassociation to the same fragment, but to the other binding site:



Of course, this reaction path has only to be considered, if the two species $FR^{(1)}$ and $FR^{(2)}$ can be distinguished electrophoretically, i.e. if their electrophoretic mobilities differ

significantly. In our calculations, we generally included path (5) to the model scheme (1). For the calculation of scheme (1) the cage effect was considered while path (5) was calculated using the normal microscopic rate constants.

Parameter values

The numerical values of the model parameters were adapted to the Tet repressor-operator system described in the experimental part of this article. The association rate constant k_a was taken from Kleinschmidt *et al.* (21): $k_a = 3 \times 10^8 \text{ M}^{-1} \text{ s}^{-1}$. The dissociation rate constant k_d which can vary over orders of magnitude with different salt concentrations, was systematically changed in our calculations in order to show the resulting effects. The starting concentrations in the gels were always $[R]^{\text{tot}} = [F]^{\text{tot}} = 1 \times 10^{-6} \text{ M}$ where the index $^{\text{tot}}$ denotes the sum of concentrations of the free and complexed species. Since a fragment contains two operators, the total operator concentration is twice the total repressor concentration. This choice ensures the simultaneous presence of free as well as single and double occupied fragments and is, thus, most instructive. Moreover, it represents the experimental situations set up to verify the results of the model calculations. The gel cage escape rate constant $k_3 = 4.4 \times 10^5 \text{ s}^{-1}$ is taken from Cann (3) and is assumed to be independent on the polyacrylamide concentration. The electrophoretic mobilities of all species were experimentally determined. Two data sets were used for two different gel concentrations: 1.) 5% polyacrylamide: F : $407 \mu\text{m/s}$, $\text{FR}^{(1)}$ = $\text{FR}^{(2)}$: $289 \mu\text{m/s}$, FR_2 : $228 \mu\text{m/s}$, R : $200 \mu\text{m/s}$. 2.) 10% polyacrylamide: F : $88 \mu\text{m/s}$, $\text{FR}^{(1)}$: $38 \mu\text{m/s}$, $\text{FR}^{(2)}$: $34 \mu\text{m/s}$, FR_2 : $20 \mu\text{m/s}$, R : $15 \mu\text{m/s}$. These data were determined in gel mobility experiments at an electric field of 6.25 V/cm . The

positions of the free repressor are visualized by Coomassie blue staining of the gels in addition to the usual detection of DNA bands with ethidium bromide.

Computer calculations

All numerical calculations were performed on a Convex C201 vectorizing computer. The program was written in Fortran and used double precision arithmetics throughout. The gel was simulated in the computer by five arrays which contained the concentration of the five reaction species. The length of the arrays was up to 120000 storage registers each representing a gel slice with a fixed thickness of $1 \mu\text{m}$ towards the anode. Thus, a maximal gel length of 12 cm could be calculated. In the beginning a fixed number of slices (1000 = 1 mm for 5% gels, 500 = 0.5 mm for 10% gels) was occupied by the constituents at the specified concentrations in *chemical equilibrium*. The gel run was simulated by the iterative, alternating execution of one movement and one reaction step. The time interval between two iterations was adjusted so that the slowest component moved $5 \mu\text{m}$ (= 5 slices) in one step. If the mobility of a component resulted in a non-integral number of slices per iteration, a random generator was used in each step to pick one of the neighboring integers. The reaction part of each iteration was evaluated in a sub-iteration. The time interval was dynamically adjusted so that the concentration change for all species was below 10 percent in each step. After completion of a simulation, the number of data was reduced to about 800 slices by averaging neighboring values. These data were used for the plots. Diffusion was generally neglected in the calculations, since its effects are small compared with electrophoretic mobility and do not provide any additional information.

RESULTS AND DISCUSSION

Titration of *tet* regulatory DNA fragments from classes A and B with class B Tet repressor

Titration experiments of 86 bp and 80 bp DNA fragments containing the class A and B *tet* regulatory sequences, respectively, with the class B Tet repressor analyzed by mobilities on 5% polyacrylamide gels are shown in Fig 1. Since each DNA fragment contains two *tet* operators, repressor-DNA complexes with two different stoichiometries can be formed. Both of them and the free DNA are indeed observed in the reaction of class B Tet repressor with class B *tet* operator DNA. When the molar

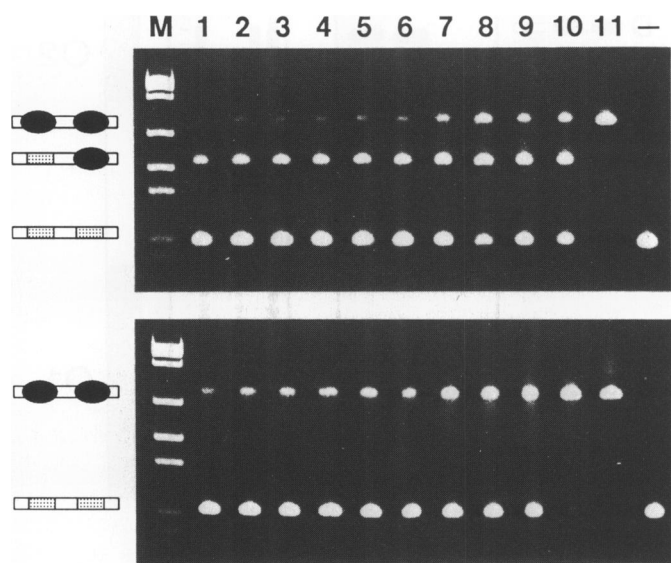


Fig. 1. Titration experiment of *tet* control DNA fragments of classes A and B with Tet^B repressor. The reaction mixtures were electrophoresed in 5% polyacrylamide gels at 2.5 V/cm for 12 hours. The total DNA concentration in each lane is $9 \times 10^{-7} \text{ M}$. The rightmost lane in the upper gel contains the free 80 bp class B *tet* DNA fragment and the rightmost lane of the lower gel the free 86 bp class A *tet* DNA fragment. Lanes 1 to 11 contain the same DNA fragments and increasing amounts of class B Tet repressor protein. The concentrations given in 10^{-7} M repressor dimer are, from lane 1 to 11: 1.1; 2.2; 2.4; 2.7; 3.1; 3.7; 4.4; 5.5; 7.3; 11; 22. Lane M shows a molecular weight standard. The sketch on the left side indicates the free DNA with the *tet* operators (shaded boxes) and the complexes with either one or two Tet repressor proteins (black ellipsoids).

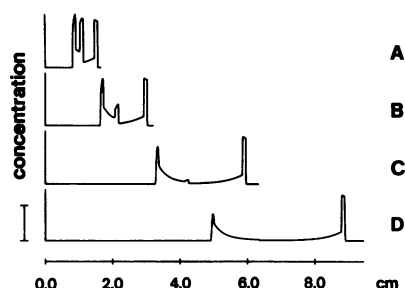


Fig. 2. Simulation of the band patterns in a 5% polyacrylamide gel obtained after different running times. The curves show the total fragment concentration (i.e. $[F]^{\text{t}} = [F] + [\text{FR}^{(1)}] + [\text{FR}^{(2)}]$) which is usually seen in an experimental gel after staining with ethidium bromide in dependence of the distance to the starting point. Times of electrophoresis: A: 1h, B: 2h, C: 4h, D: 6h, $k_d = 1 \times 10^{-1} \text{ s}^{-1}$. For the other parameters see Materials and Methods section. The length of the bar marks a concentration of $2 \times 10^{-7} \text{ M}$.

ratio of protein to DNA is low only the complex with one operator occupied by repressor is present. The two different occupations of the neighboring operators cannot be distinguished. When the molar ratio of Tet repressor dimer to DNA approaches one the complex with both operators bound shows up and becomes more prominent upon adding more repressor. This result indicates independent binding of repressor to the two operator sites and agrees with quantitative thermodynamic and kinetic studies (21).

A different distribution of free and complexed DNA is found when class A *tet* regulatory DNA is titrated with the class B repressor (see Fig. 1). In this case the band corresponding to the occupation of only one *tet* operator by one Tet repressor dimer is not observed. Only the band corresponding to the double occupation is visible and shows an increased intensity. This distribution of complexes is often interpreted as cooperative

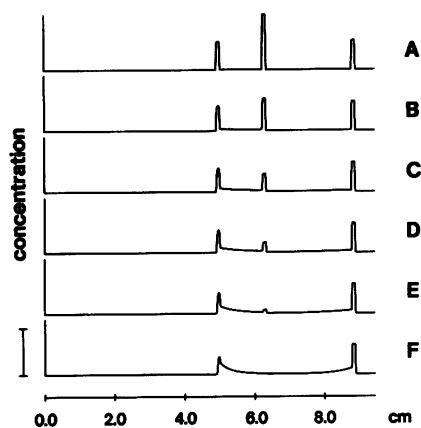


Fig. 3. Same as Fig.2, but with fixed running time of 6h and different dissociation rate constants k_d [s^{-1}]: A: 1×10^{-3} , B: 1×10^{-2} , C: 2×10^{-2} , D: 3×10^{-2} , E: 5×10^{-2} , F: 1×10^{-1} . The length of the bar is 4×10^{-7} M.

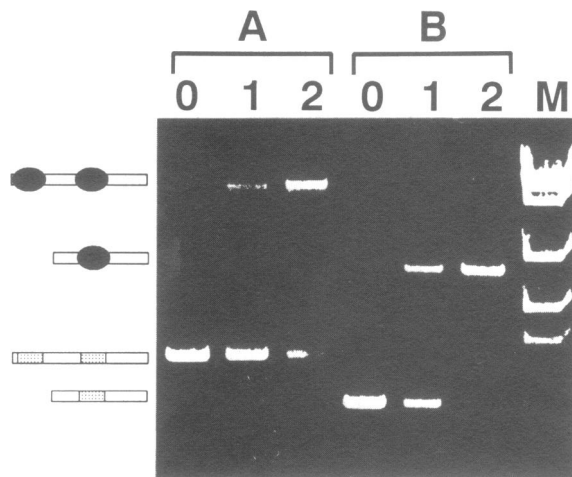


Fig. 4. 5% polyacrylamide gel analysis of class A Tet repressor interaction with single and multiple class B *tet* operators on a DNA fragment. A 124 bp DNA containing the *tet* operators O_1 and O_2 with a *Bgl*III site between them is loaded in part A lane 0. The same DNA is loaded after *Bgl*III digestion in part B lane 0. The smaller fragment is lost in the gel. The concentration of operators in all lanes is 2.8×10^{-7} M. In lanes 1 class A Tet repressor was added at 2×10^{-7} M and in lanes 2 at 4×10^{-7} M. Lane M contains a molecular weight marker. The sketches on the left indicate the free and complexed DNA species contained in the respective bands.

binding. Since different binding modes of Tet repressor to similar substrates is not very likely, we applied the theoretical scheme (see in Materials and Methods) to simulate the mobility of DNA fragments with two identical operators on 5% polyacrylamide gels in the presence of the binding protein. The electrophoretic mobilities of both single occupied fragments $FR^{(1)}$ and $FR^{(2)}$ are taken to be identical. Fig. 2 shows the resulting band patterns of a simulation of an equimolar mixture of protein and DNA with a fixed dissociation rate k_d in dependence of time. At the beginning, three bands representing the free, singly and doubly complexed fragments are present. At later times of gel electrophoresis, the middle band representing $FR^{(1)}$ and $FR^{(2)}$ gradually disappears, whereas the trailing band of doubly occupied fragment FR_2 is much more, although not entirely, stable. Only the intensity of the leading band representing the free DNA remains unchanged. Since the repressor has the lowest mobility of all species no reactions can take place at this position in the gel. The gradual disappearance of the middle band is accompanied by a smearing, which can indeed often be seen in respective experiments (compare below). Note that the fully developed gel (Fig. 2, lane D) corresponds to the result obtained in the titration experiment of class A DNA with class B repressor in Fig. 1. The model used for the simulations is strictly non-cooperative. Thus, this result can be interpreted without assuming cooperativity.

In order to study the reason for the disappearance of the single complex species the patterns resulting from a systematic variation of dissociation rate constants were simulated. In Figure 3 the band

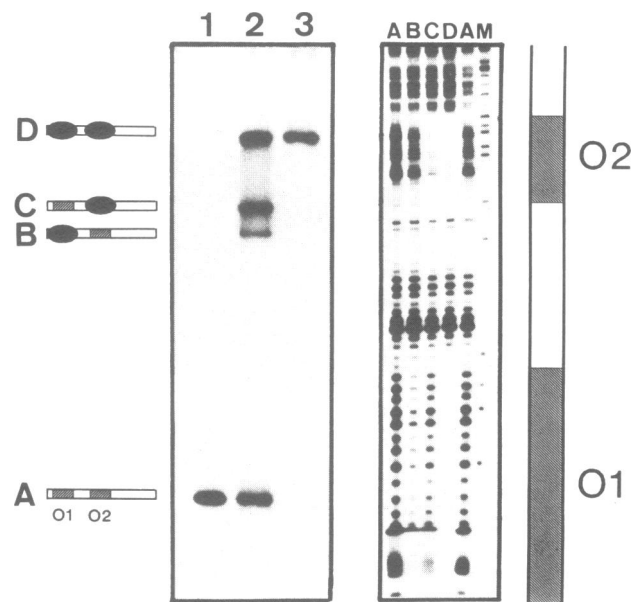
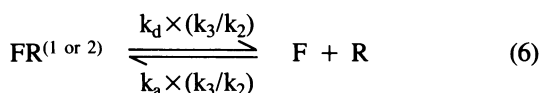
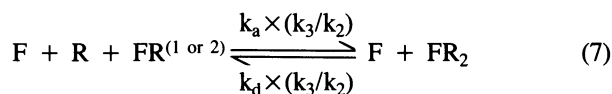


Fig. 5. Separation and assignment of different repressor-operator complexes. At the left side an autoradiograph of a native 10% polyacrylamide gel is shown. The 112 bp fragment, described in Materials and Methods, containing the two *ter*^B operators, O_1 at the end of the fragment, and O_2 in the middle of the fragment was electrophoresed after incubation with various amounts of *Tet*^B repressor. Lane 1 contains the free fragment and the ratio of repressor to operator concentration is in lane 2 0.5 and in lane 3 5.0. The resulting DNA bands, indicated as in Fig 1 and designated A to D, were footprinted in the gel matrix. The DNA was eluted from the gel and separated on the sequencing gel shown on the right. The DNA sequence was assigned by comparison to the bands in lane M, where the products of the guanine-specific sequencing reaction were separated. The positions of the *ter*^B operators O_1 and O_2 on the DNA fragment are indicated at the right side as dark boxes.

patterns of fully developed gels are shown for dissociation rate constants varying between $1 \times 10^{-3} \text{ s}^{-1}$ and $1 \times 10^{-1} \text{ s}^{-1}$. For the lowest k_d (lane A) a typical pattern for the limit of strong binding can be seen: three bands with a density ratio of 1:2:1. This corresponds to the results observed for the class B *tet* regulatory DNA titrated with the class B Tet repressor in Fig. 1. Although k_d in lane A ($1 \times 10^{-3} \text{ s}^{-1}$) is much larger than the reciprocal running time ($4.63 \times 10^{-5} \text{ s}^{-1}$), the bands are stable because of the cage effect. The quantity determining the band stability is the macroscopic dissociation rate, which is obtained according to eq. (4) by multiplication of k_d with the factor k_3/k_2 ($= 1.47 \times 10^{-3}$ for our parameter values). E.g., in lane D the macroscopic dissociation rate is $3 \times 10^{-2} \text{ s}^{-1} \times 1.47 \times 10^{-3} = 4.4 \times 10^{-5} \text{ s}^{-1}$, which approximately equals the reciprocal electrophoresis time and apparently represents the borderline between stability and decay of the middle band. On the contrary, the band of the doubly occupied fragment FR_2 is unexpectedly stable leading to the apparent 'cooperative' two-band-distribution. An explanation for this phenomenon is derived from a detailed inspection of the reactions involved in each band. In the middle band containing mainly the two species $\text{FR}^{(1)}$ and $\text{FR}^{(2)}$ the dissociation according to the following equation (here written with the retarded rate constants):



is accompanied by either the reassociation according to eq. (6) or a complexation of the free repressor molecule with an already singly occupied fragment:



Eq. (6) and (7) can be summarized to an effective 'disproportionation' reaction



Since the 'choice' of the two reassociation possibilities of the free repressor (eq. (6) or eq. (7)) is of a purely statistical nature, it is independent of k_a and k_d and, thus, on the binding constant

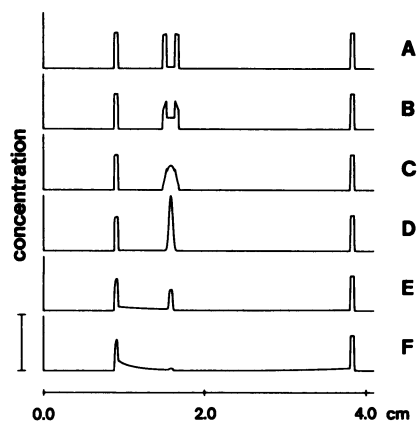
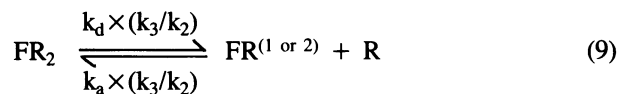


Fig. 6. Calculated band patterns in a 10% polyacrylamide gel assuming that $\text{FR}^{(1)}$ and $\text{FR}^{(2)}$ have different mobilities. The time of electrophoresis is 12h. The dissociation rate constants k_d are: A: 3×10^{-6} , B: 3×10^{-5} , C: 1×10^{-4} , D: 1×10^{-3} , E: 1×10^{-2} , F: $3 \times 10^{-2} \text{ s}^{-1}$. The length of the bar is: $4 \times 10^{-7} \text{ M}$.

k_a/k_d . The disproportionation rate of eq. (8) is simply dependent on the rate of appearance of free repressor, i.e. $k_d \times (k_3/k_2)$. A disproportionation without escape from the gel cell is not possible since a polyacrylamide gel pore contains at the most one DNA fragment. Therefore, during the gel run the amount of the FR species decreases. The rate of this process is just a function of k_d and formally independent of the total binding strength.

On the other hand, the band of the doubly occupied fragment FR_2 can dissociate as follows:



However, since R can only reassociate according to the same equation (the concentration of the free fragment F is assumed to be negligible), no 'statistical' disproportionation can occur. The only possible mechanism for the decay of the FR_2 band is the electrophoretic separation of the species FR and R before reassociation. This process depends on the association rate k_a and, thus, on the binding constant as well as on the electrophoretic mobilities. A high binding strength will prevent loss of the FR_2 species regardless of the value for k_d . A detailed analysis of Tet repressor-*tet* operator association has shown that two steps are involved in this reaction (21). However, the mechanism of association does not influence the results derived here.

According to these considerations the lack of the singly occupied complex is due to disproportionation of the complex during gel electrophoresis and not to an inherent instability of the single complex. The experimental verification for this conclusion is shown in Fig. 4. The class B *tet* operator class A Tet repressor mixture yields only two bands, one corresponding to the free DNA and one containing the doubly occupied DNA. No DNA with single *tet* operator occupation is detectable.

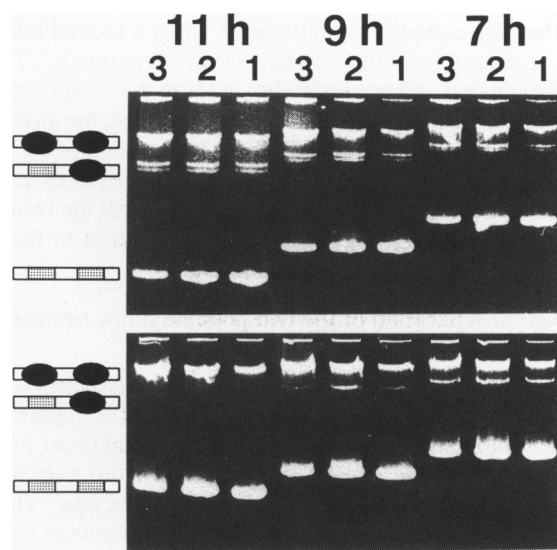


Fig. 7. Comparison of a gel shift experiment using Tet^B repressor protein and tet^B operator DNA in gel systems of different ionic strengths. Reaction mixtures containing $9 \times 10^{-7} \text{ M}$ of the 80 bp class B *tet* DNA fragment and $7 \times 10^{-7} \text{ M}$ (lanes 1), $1 \times 10^{-6} \text{ M}$ (lanes 2) and $1.4 \times 10^{-6} \text{ M}$ (lanes 3) of Tet^B repressor dimer were loaded at different times onto the two shown 10% polyacrylamide gels. The separation times were, as indicated above 7, 9 or 11 hours at constant voltages of 6.25 V/cm. The buffer of the gel at the bottom contained 40 mM sodium chloride in addition to the buffer used for the gel shown above.

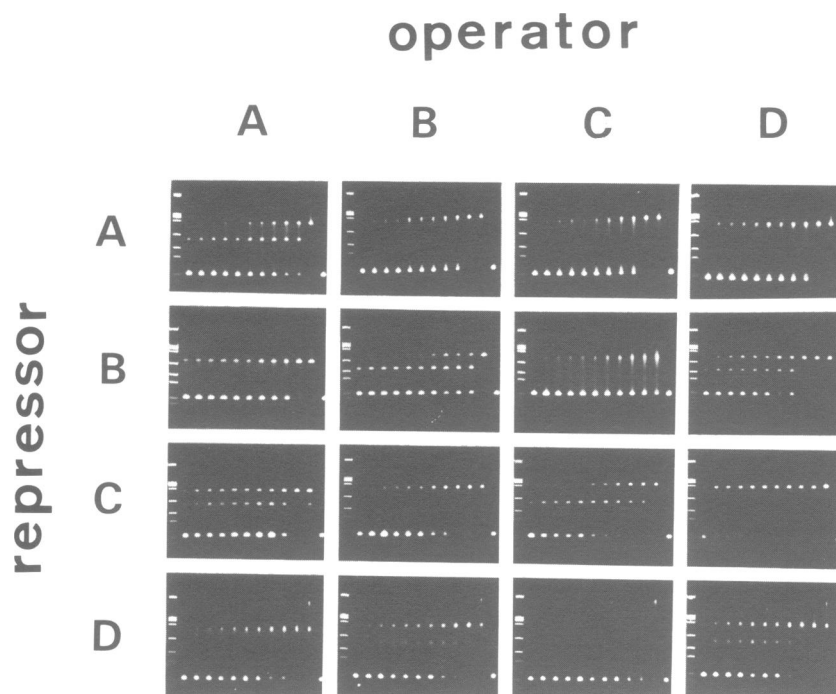


Fig. 8. Titration of four *tet* DNA fragments with four different Tet repressor proteins of the resistance classes A, B, C, and D. Titration experiments of *tet* DNA fragments with Tet repressor proteins of the four classes are analysed by electrophoresis in 5 per cent polyacrylamide gels as described in Fig. 1. The gels in each column contain the same *tet* fragments of the classes indicated above with lengths of 86 bp (class A), 80 bp (class B), 84 bp (class C), and 78 bp (class D) and they were titrated in the gels of each row with the same repressor proteins of *tet* classes denoted at the left. The total concentration of DNA fragments in each lane of all gels is 9×10^{-7} M. The rightmost lanes in each gel contain the free DNA fragments. The following lanes to the left contain decreasing amounts of the repressor proteins. The repressor concentrations given in 10^{-7} M dimer are, from right to left for Tet^A repressor (0; 24; 12; 8; 6; 4.8; 4.0; 3.4; 3.0; 2.6; 2.4; 1.2), for Tet^B repressor (0; 22; 11; 7.3; 5.5; 4.4; 3.7; 3.1; 2.7; 2.4; 2.2; 1.1), for Tet^C repressor (0; 21; 10.5; 7.0; 5.2; 4.2; 3.5; 3.0; 2.6; 2.3; 2.1; 1.1), and for Tet^D repressor (0; 30; 15; 10; 7.5; 6.0; 5.0; 4.3; 3.8; 3.3; 3.0; 1.5).

However, when the DNA fragment is digested with *Bgl*III yielding a large and a small DNA fragment with one *tet* operator each, the complex with Tet repressor is stable in the gel. This indicates clearly that this complex is only absent when a second binding site is present on the same DNA fragment. Thus, disproportionation and not instability leads to the disappearance of this species. Disproportionation may also explain the increased intensity of the doubly occupied DNA in the titration of the class A operator fragment in Fig. 1. This may be the result of a rapid dissociation of the singly occupied complex, so that the resulting doubly occupied DNA migrates at a position close to the one of the complex formed by direct binding.

Experimental separation of the two possible single *tet* operator occupations

The results of the calculations imply that the dissociation rate of the homologous complex is very small, while it is much larger for the heterologous complex. Direct experimental proof for the small dissociation rate can be obtained when the two singly occupied *tet* operator complexes can be distinguished. This is realized by the construction of a 112 bp DNA fragment (see in Materials and Methods) having one *tet* operator O_1 close to an end of the fragment, while the other *tet* operator O_2 is located in the middle of the fragment. Due to repressor induced bending of the operator DNA the complex at the end has a greater mobility on a 10% polyacrylamide gel than the one with the bend in the middle (22). The autoradiograph in Fig. 5 shows the gel obtained with this DNA in the presence of Tet repressor. It displays indeed two separated bands corresponding to the single occupation of each *tet* operator. This interpretation of the band pattern is proven

by footprinting the repressor-DNA complexes in situ. The result is also shown in Fig. 5. Lane A contains a footprint of the free DNA showing no protection. Lane B shows the footprint of the complex B showing only protection of the *tet* operator at the end of the fragment. Lane C shows the footprint of complex C showing only protection of the middle *tet* operator. In lane D the doubly occupied fragment is footprinted showing protection of both *tet* operators. This experiment shows unambiguously that very little dissociation occurs during the electrophoresis. Furthermore, it confirms that the affinity of Tet repressor for *tet* operator O_2 (middle) is about 5-fold higher than the one for *tet* operator O_1 (end) (23). Thus, the implication of the computer simulations that a low apparent dissociation rate leads to the appearance of the singly occupied species on polyacrylamide gels is confirmed by these experiments.

Influence of the dissociation rate on the separation of the two single *tet* operator occupations

In the next simulations the apparent gel patterns for complexes of a DNA fragment containing two binding sites were determined as a function of the dissociation rate assuming that the two single complexes have different mobilities. For the sake of simplicity it was assumed that both binding sites have identical affinities for the binding protein. The results for dissociation rate constants varying between $3 \times 10^{-6} \text{ s}^{-1}$ and $3 \times 10^{-2} \text{ s}^{-1}$ are displayed in Fig. 6. An interesting biphasic behavior can be observed. In the first phase (lane A to D) the primarily separated bands $FR^{(1)}$ and $FR^{(2)}$ merge, until they form a common but stable band. In the second phase (lanes D to F) this band disappears according to the already discussed mechanism. Note that in lane D the

reciprocal electrophoresis time ($2.31 \times 10^{-5} \text{ s}^{-1}$) is smaller than k_d ($= 1 \times 10^{-3} \text{ s}^{-1}$) but larger than $k_d \times (k_3/k_2)$ ($= 1.47 \times 10^{-6} \text{ s}^{-1}$). Since the time constant for the change of binding sites according to path (5) is of the order of the reciprocal unretarded k_d , the separation of the bands FR⁽¹⁾ and FR⁽²⁾ is lost $k_2/k_3 \approx 682$ times faster than the combined band itself.

From these model calculations two predictions can be tested experimentally. First, the two singly occupied class B repressor-operator complexes should merge into one single band with an increasing dissociation rate constant and, secondly, the resulting band should disappear with extended electrophoresis time (see Fig. 2). To increase the dissociation rate constant the salt concentration of the electrophoresis buffer was raised by adding sodium chloride up to 100 mM. According to previously published results describing the dependence of Tet repressor-*tet* operator dissociation rate on the concentration of NaCl this enhances the dissociation rate constant substantially (24). A gel mobility analysis of Tet repressor binding to the two *tet* operators on an 80 bp DNA fragment at low and high sodium chloride concentrations and with different electrophoresis times is shown in Fig. 7. At low salt both bands representing the two singly occupied operators on the DNA fragment are clearly stable for eleven hours of electrophoresis. At increased salt, on the other hand, even after only seven hours just a single band for the two possible occupancies is seen. After nine hours this band has decreased in intensity and after eleven hours it cannot be detected anymore. Thus, this experiment confirms precisely the predictions derived from the computer simulations.

Analysis of sixteen Tet repressor-*tet* operator complexes by gel mobility

Four classes of tetracycline resistance determinants named A through D which encode efflux proteins (5) are regulated by similar repressor-operator systems. The primary structures of the repressors show between 43% and 63% identity (8). We have studied all 16 possible combinations by gel mobility analysis. The 16 titration experiments are displayed in Fig. 8. According to the model described above the intensity of the band corresponding to single occupation of one *tet* operator is related to the dissociation rate constant of the respective complex. For the class A repressor this band is only seen in the interaction with class A *tet* operator. All three other heterologous combinations are significantly less stable. If one assumes that the association rates may not vary dramatically the difference in dissociation rates would result in a respective difference in the equilibrium constants. This interpretation agrees well with previously published *in vivo* results showing that class A-class B recognition is much less efficient compared to recognition of the homologous compounds (14).

A somewhat different result is obtained for the class B Tet repressor. In this case an intense intermediate band is found in the titration of class B operator. An intermediate band with decreased intensity shows up in the titration with the class D *tet* operator. This may be interpreted as a moderately increased dissociation rate for this complex and agrees well with the fact that the class D *tet* regulatory elements are most homologous to the ones of class B. The class A *tet* operator is bound, but the dissociation rate constant of this complex is clearly increased, because no intermediate band can be detected. The complex with class C *tet* operator is even less stable as indicated by the smear of the doubly occupied complex band and the fact, that it occurs only at higher repressor concentrations.

The class C repressor forms the most stable complex with class C *tet* operator and a less stable complex with class A *tet* operator. This relates well to their similarities (8). It should be noted, however, that the class A repressor did not reflect this similarity to class C in its operator binding behavior. The class B and D *tet* operators are bound but with lower affinity as indicated by the lack of intermediate bands.

The class D Tet repressor forms the weakest complex of all four repressors with its operator as judged by the low intensity of the intermediate band. Gel analysis of the class A and B operators result only in the doubly occupied band while the class C *tet* operator is not bound at all under those conditions. Thus, the class D Tet repressor shows the worst operator recognition of all four variants. These results indicate that the gel mobility analysis of the singly occupied complex provides a quick and qualitative estimation of repressor-operator binding strength.

CONCLUSIONS

In modification of the analysis published by Cann (3) we have numerically calculated the gel mobility patterns of protein-DNA complexes for independent protein binding to two sites on the same DNA fragment. In the limit case of strong binding, namely with a dissociation rate constant smaller than the inverse electrophoresis time, the appearance of complex bands on the gel is as anticipated. However, in the case of weaker binding the disproportionation of complexes has to be considered. It leads first to a loss of distinction between the two different single occupancies. Then, either with increasing electrophoresis time or with higher dissociation rate disproportionation leads to a loss of the single occupation band. This results in a gel mobility pattern which could easily be misinterpreted as cooperative binding of the compounds analyzed. Of course, our simulations do not rule out cooperativity in the *tet* system. In fact, with cooperativity the results would be virtually indistinguishable from our calculated patterns. The important conclusion is, however, that cooperativity is not needed to explain these gel shift results. This should be kept in mind since multiple binding sites on the same DNA often occur e.g. for IHF or RNA polymerase (24, 25) which bind weaker to their respective binding sites or promoters than most repressors to their cognate operators. Furthermore, eukaryotic transcription factors often have multiple binding sites in a given regulatory region. Our analysis shows that it may not be straightforward to interpret gel mobility shift experiments in these cases.

ACKNOWLEDGEMENTS

The authors wish to thank A.Rehm and A.Wissmann for construction of the *tet* operator distance mutant and K.Garke for typing the manuscript. This work was supported by grants from the Deutsche Forschungsgemeinschaft, the BMFT and the Fonds der chemischen Industrie.

REFERENCES

1. Garner, M. M. and Revzin, A. (1981) *Nucleic Acids Res.* **9**, 3047–3060
2. Fried, M. G. and Crothers, D. M. (1981) *Nucleic Acids Res.* **9**, 6505–6525
3. Cann, J. R. (1989) *J. Biol. Chem.* **264**, 17032–17040
4. McMurray, L., Petrucci, R. E. and Levy, S. B. (1980) *Proc. Nat. Acad. Sci. USA* **77**, 3974–3977
5. Mendez, B., Tachibana, C. and Levy, S. B. (1980) *Plasmid* **3**, 99–108
6. Marshall, B., Morrissey, S., Flynn, P. and Levy S. B. (1986) *Gene* **50**, 111–117

7. Unger, B., Becker, J. and Hillen, W. (1984) *Gene* **31**, 103–108
8. Unger, B., Klock, G. and Hillen, W. (1984) *Nucleic Acids Res.* **12**, 7693–7703
9. Postle, K., Nguyen, T. T. and Bertrand, K. P. (1984) *Nucleic Acids Res.* **12**, 4849–4863
10. Waters, S., Rogowsky, P., Grinstead, J., Altenbuchner, J. and Schmitt, R. (1983) *Nucleic Acids Res.* **11**, 6089–6105
11. Tovar, K., Ernst, A. and Hillen, W. (1988) *Mol. Gen. Genet.* **215**, 76–80
12. Bertrand, K. P., Postle, K., Wray, V. Jr. and Reznikoff, W. S. (1983) *Gene* **23**, 149–156
13. Hillen, W., Klock, G., Kaffenberger, I., Wray, L. V. and Reznikoff, W. S. (1982) *J. Biol. Chem.* **257**, 6605–6613
14. Klock, G., Unger, B., Gatz, C., Hillen, W., Altenbuchner, J., Schmid, K. and Schmitt, R. (1985) *J. Bact.* **161**, 326–332
15. Altschmied, L., Baumeister, R., Pfeleiderer, K. and Hillen, W. (1988) *EMBO J.* **7**, 4011–4017
16. Tovar, K. and Hillen, W. (1990) *Methods in enzymol.* in press
17. Klock, G. and W. Hillen (1986) *J. Mol. Biol.* **189**, 633–641
18. Oehmichen, R., Klock, G., Altschmied, L. and Hillen, W. (1984) *EMBO J.* **3**, 539–543
19. Wissmann, A., Meier, I. and Hillen, W. (1988) *J. Mol. Biol.* **202**, 397–406
20. Kuwabara, M. D. and Sigman, D. S. (1987) *Biochemistry* **26**, 7234–7238
21. Kleinschmidt, C., Tovar, K., Hillen, W. and Pörschke, D. (1988) *Biochemistry* **27**, 1094–1104
22. Tovar, K. and Hillen, W. (1989) *Nucleic Acids Res.* **17**, 6515–6521
23. Hillen, W., Gatz, C., Altschmied, L., Schollmeier, K. and Meier, I. (1983) *J. Mol. Biol.* **169**, 707–721
24. Robertson, C.A. and Nash, H.A. (1988) *J. Biol. Chem.* **263**, 3554–3557
25. Ogden, S., Haggerty, D., Stoner, C.M., Kolodrubetz, D. and Schleif, R. (1980) *Proc. Natl. Acad. Sci. U.S.A.* **77**, 3346–3350
26. Cann, J.R. and Goad, W.B. (1965) *J. Biol. Chem.* **240**, 148–155
27. Cann, J.R. (1987) *J. Theor. Biol.* **127**, 461–677